Numerical analysis of track: Structure interaction and time domain resonance

M Petrangeli, C Tamagno and P Tortolini

Proceedings of the Institution of Mechanical Engineers, Part F: Journal of Rail and Rapid Transit 2008 222: 345
DOI: 10.1243/09544097JRRT168

Numerical analysis of track: structure interaction and time domain resonance

M Petrangeli, C Tamagno*, and **P Tortolini**
University of Pescara, Integra, Rome, Italy

The manuscript was received on 3 July 2007 and was accepted after revision for publication on 26 March 2008.

DOI: 10.1243/09544097JRRT168

Abstract: This paper illustrates the mechanics of track–structure interaction and resonance, and the finite-element (FE) modelling of railway girders subjected to combined live and thermal loadings. The numerical analysis makes use of the recent insertion of a ballast FE into the FE code FIBRE. The element complies with the Italian railway specifications and has been tested and validated accordingly. The program, originally developed to model the seismic (dynamic) response of civil structures, can perform step-by-step non-linear analyses in the time domain using a state-of-the-art library of fibre beam-column elements and other bridge dedicated FEs such as frictional bearing, gap, tendons, etc. Following the implementation of the ballast element, the non-linear static and dynamic responses of railway bridges can be analysed considering the track–structure interaction effects. With the same FE mesh, temperature effects, quasi-static, and dynamic (resonant) response under live loading as well as seismic response of bridge structures can now be analysed with a unified approach. In all these cases, the continuous welded rail significantly modifies the response of railway bridges, especially in the small to medium span range. After discussing the new ballast FE, a numerical case study is presented showing all the different types of analyses that can be performed with the program. The principal mechanisms governing the response of railway girders and bridges are discussed showing the stress–strain time histories of the principal bridge elements.

Keywords: track–structure interaction, ballast behaviour, finite-element non-linear analysis

1 INTRODUCTION

Rail expansion joints are hardly found along the Italian railway network and usage of such joints is discouraged due to its maintenance requirements. Especially when it comes to bridges, these are specifically designed so as to avoid rail joints. This approach is one of the reasons for the extended use of simply supported beams with limited length between adjacent deck expansion joints. It also discourages the realization of high performance continuous or cable-supported structures or slender and more appealing sub-structures unless reliable numerical simulations can be performed to assess the forces that may arise into the continuous welded rail (CWR). These forces arise mostly due to temperature effects and seismic loading, where applicable, but also live loading and breaking or accelerating forces can be of a certain relevance.

Since all these phenomena are highly non-linear, a single numerical tool to deal with all is required as stress superposition is generally not applicable. Once a reliable tool is available, the application of the CWR can be possibly extended to longer bridges as the stresses in the rails are easily controlled and the track itself may have some positive effect on the bridge structural behaviour.

At present, track–structure interaction and resonance analyses are required by the Italian Norms [**1**] for any bridge that does not fall within specified limits. These limits are basically the maximum span length (around 30 m for reinforced and prestressed concrete) and stiffness of piers and foundations that must be particularly high and evenly distributed among different supports. When bridges fall within these specified limits, equivalent linear elastic analyses can be

**Corresponding author: University of Pescara, Integra, Via di s Erasmo 16, 00184 Rome, Italy. email: www.integer.it*

performed. Outside these bounds, non-linear step-by step analyses are required to assess the track–structure interaction [**2**].

General purpose finite-element (FE) program can sometimes be used although not directly as both the load input and the ballast behaviour are not readily available in the most convenient form. Awkwardness in the load input is the major cause of concern in resonance analyses since a large spectrum of loading histories needs to be investigated. Ballast constitutive behaviour, vice versa, can be the problem in track–structure interaction analyses since the specific constitutive behaviour may be difficult to obtain using available simplified non-linear models.

2 THE FIBRE FE PROGRAM

FIBRE is a three-dimensional non-linear FE program for the analysis of civil structures. The program has been developed in the last 15 years from the family of codes known as DRAIN3D and ANSR [**3**]. Developments have addressed different aspects of structural engineering, with most notable achievements obtained in the field of non-linear response of framed structure [**4**, **5**]. The non-linear fibre element with fibre shear modelling available in the program [**5**] can be used for the post-elastic analysis of bridges and other railway structures subjected to live and seismic loads. Shear capabilities are particularly useful in railway engineering as squat piers and deep beams are very common among railway structures.

The need for non-linear analysis of structures has also received a major acceleration by the introduction of the new European Norm [**6**, **7**] and more recently by the new 'Displacement Based Approaches' [**8**, **9**].

It was therefore decided to upgrade the program with necessary features to carry out the interaction and resonance analyses as well. It is now possible to perform with the same model and program all the above-said types of analyses, including large displacement and buckling analysis as the program uses a total Lagrange formulation.

3 THE BALLAST CONSTITUTIVE BEHAVIOUR

The Italian Railway Norm [**1**] define the ballast response under horizontal loading with a family of elastoplastic force–displacement curves (Fig. 1) with a constant yield displacement (Δ_y) of 2 mm and a yield force (F_Y) linearly dependent on the axial load (N) as follows

$$F_Y(N) = F_{\min} + \Phi N \tag{1}$$

The friction coefficient Φ and the minimum friction force $F_{\min}$ being set to 0.5 and 20 kN/m on bridge deck

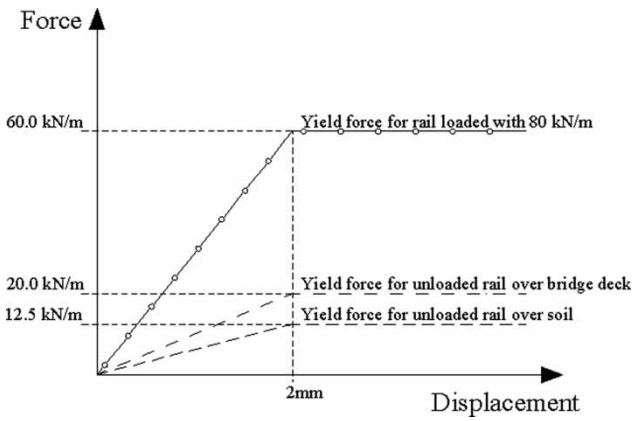

Fig. 1 Ballast force–displacement curves

and 0.594 and 12.5 kN/m on soil, as shown in Fig. 1. The axial behaviour is assumed to be linear elastic with stiffness equal to 130 MN/m/m. Other parameters, which are not explicitly specified in the Norm have been assumed as follows.

(a) Unloading is linear-elastic, with the modulus being a function of the axial load;
(b) Tangent modulus $K(N)$ for loading, reloading, and unloading branches (the implemented constitutive behaviour has full cyclic capabilities) is found with the following expression;

$$K(N) = \frac{F_Y(N)}{\Delta_y} \tag{2}$$

(c) the friction behaviour is fully two-dimensional.

It should be pointed out that the assumption used to define the tangent modulus is one out of a number of other available options. As a matter of fact, the variable stiffness found using equation (2) could not be obtained by putting in series a linear-elastic element with a frictional element. Another worth noticing feature of the proposed model is that the axial force influences the shear yielding force, while the shear response does not influences the axial one. This is a gross approximation as generally granular materials show a very strong dilatancy when subjected to shear forces. Nonetheless the vertical behaviour of the ballast-rail system has negligible effects on the bridge response, as the load applied to the rail (train loading) is largely independent of its vertical response.

4 THE BALLAST FE

The ballast FE is a shear only type of element with six nodes and six degrees of freedom. The vector of nodal displacements is

$$\boldsymbol{U}^e = (U_x^i \;\; U_y^i \;\; U_z^i \;\; U_x^j \;\; U_y^j \;\; U_z^j)^{\mathrm{T}} \tag{3}$$

The element is based on a displacement approach where the element generalized deformation $\varepsilon^{\mathrm{e}} = (\Delta_{\mathrm{x}}\Delta_{\mathrm{y}}\Delta_{\mathrm{z}})^{\mathrm{T}}$ (the axial elongation and the two generalized distortions perpendicular to the element axis) are found multiplying the vector of nodal displacements by the compatibility matrix **D**

$$\varepsilon^{\mathrm{e}} = \mathbf{D}\boldsymbol{U}^{\mathrm{e}} \tag{4}$$

where **D**, for a local element system parallel to the global (nodal) reference system, can be written as follows

$$\mathbf{D} = \begin{vmatrix} -1 & 0 & 0 & 1 & 0 & 0 \\ 0 & -1 & 0 & 0 & 1 & 0 \\ 0 & 0 & -1 & 0 & 0 & 1 \end{vmatrix} \tag{5}$$

Once deformations are computed, the generalized stresses $\sigma^{\mathrm{e}} = (N\ T_{\mathrm{y}}\ T_{\mathrm{z}})$ are found with the constitutive behaviour discussed earlier. The possibility of a tension cut-off in the ballast axial response is also available so as to account for rail and truck buckling. Once the stresses are known, the nodal forces $\boldsymbol{F}^{e} = (F_x^i\ F_y^i\ F_z^i\ F_x^j\ F_y^j\ F_z^j)^{\mathrm{T}}$ are found using the transpose of **D** matrix. Since the element neither has rotational degrees of freedom nor associated bending forces, it does not satisfy equilibrium if a non-zero length is specified. For practical purpose though, the program does accept non-zero length ballast elements as this may sometimes simplify the input file introducing an error.

5 MOVING LOAD GENERATION

Both interaction and resonance analyses require a number of different trains to be generated and applied over the structure. For the interaction analysis, the Italian Norms require the same trains used in static analysis such as the standard LM71 (UIC71), SW/0 and SW/2 [**1**]. For the resonance analysis, five different trains are to be used instead. Each of them is to be applied over a range of velocities up to the specified maximum that varies from 200 to 350 km/h at an increment of 10. Given the large amount of loading histories to be generated, the program was enriched with automatic generation capabilities. These capabilities allow for the description of any generic train as an unlimited series of point and distributed loads moving along the bridge at a specified speed.

6 A CASE STUDY

The large prefabricated twin-box deck found along the new high-speed railway line Turin-Milan [**10**, **11**] has been used for the case study. The deck is made of two separately prefabricated box girders weighing over 400 t each. By joining two of these girders together, a deck of 13.6 m width and 34.5 m gross span is made (Fig. 2). Over 250 of these girders have been used along the above-said line.

Although this type of girder has been used for long viaducts, the proposed case study applies, for the sake of simplicity and clarity, to a single span. Sub-structures are supposed to have an horizontal stiffness of 100 MN/m/m which roughly correspond to that of a short abutment/pier. Other geometric and mechanical characteristics are given in Table 1.

6.1 The FE model

The analyses have been performed for half deck (a single box-girder) with a two-dimensional model (Fig. 3). By doing this, minor transverse and torsional effects are neglected. In the interaction analysis it is fundamental to place each element in its exact vertical

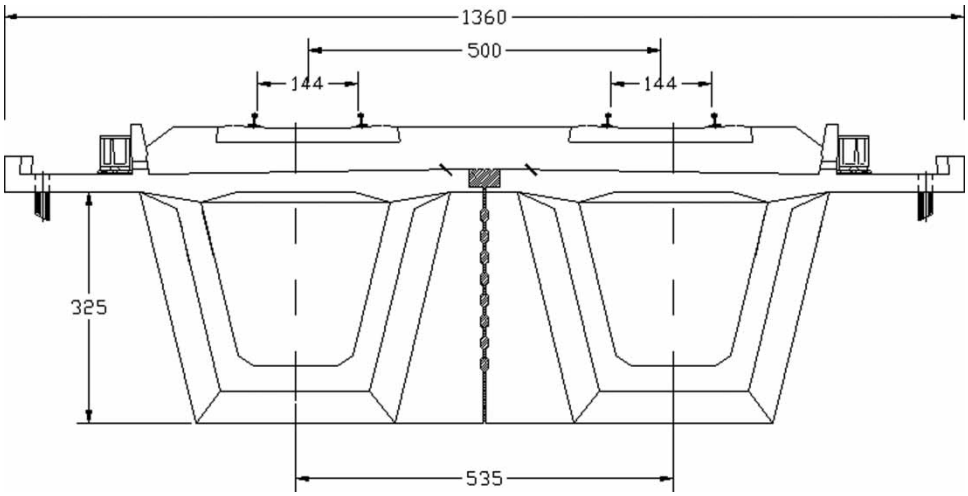

Fig. 2 The twin-box girder cross-section

Table 1 Geometric and mechanical characteristics

Rail area	76.9 cm^2
Rail vertical inertia	3055 cm^4
Ballast thickness	0.35 m
Distance between box girder and rail axis	1.68 m
Distance between box girder axis and support	4.22 m
Box girder vertical inertia	5.95 m^4
Self weight and permanent load for a complete span	7500 kN

position. The deck beam elements have been therefore placed at the deck axis level and so for the rail elements. Rigid links connect the deck elements to the supports. Rigid links in series with ballast elements connect the deck to the rail elements. Further details on the deck rail connections are given in the next section.

Except for the ballast elements, the linear elastic behaviour has been assumed for all other bridge elements. According to the Italian Norms, the rail has been extended for 100 m in both directions beyond the bridge abutments assuming the line runs on embankment (ballast on ground). Total length of the model is therefore 234.5 m; the abscissa starts on the left. The sliding support, on the left, is therefore placed at abscissa $x = 100$ m, the fixed support, on the right, at abscissa $x = 133.1$ m. Node spacing for the deck and rail has been set equal to the sleeper spacing, which is 0.6 m. This very close node spacing, with respect to the bridge (span) length, may be computationally too demanding. A larger spacing can be used without incurring in a significant loss of numerical accuracy. In this case, though the rail flexural inertia must be scaled accordingly, as explained in the following paragraph.

6.2 Modelling of deck–rail connection

The connection between the bridge deck and the rail is made of three components; the rail–sleeper joint, the sleeper itself and the ballast. As far as the shear behaviour is concerned, the response is governed by the ballast since the other two elements can be considered completely rigid. When it comes to bending in the vertical plane, neither the rail–sleeper joint nor the sleeper–ballast contacts are rigid compared to the rail flexural inertia. Bending moments caused by the axially loaded rail will therefore distribute differently depending on the relative stiffness of these three elements.

Since the actual stiffness of the rail–sleeper joint and sleeper–ballast contact may depend on a number of different factors including maintenance and live loading – sleepers loaded by the train are stiffer to tilt – both a pin (zero stiffness) and a built-in (totally rigid) connection has been assumed for the two mechanisms, as shown in Fig. 4.

When a fixed connection is used, results show that the point of contra flexure tends to occur very closely to the rail and thus the rail is not subjected to significant bending forces. When, vice versa, a pin connection is used, bending moment will arise in the rail equal to the product of the shear force carried by the ballast

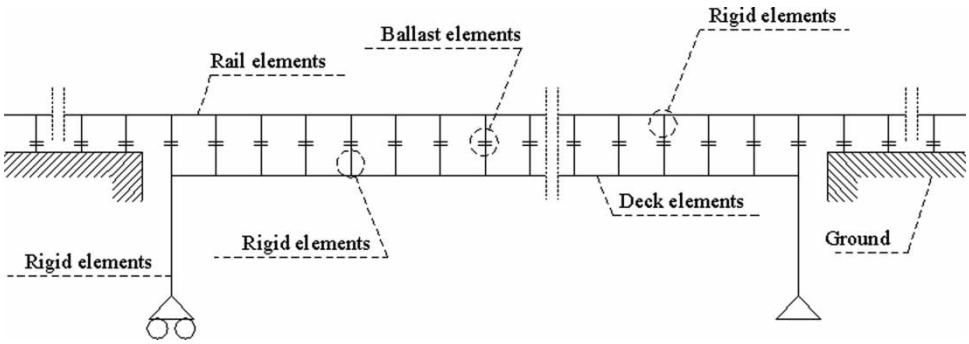

Fig. 3 Overview of the two-dimensional FE model

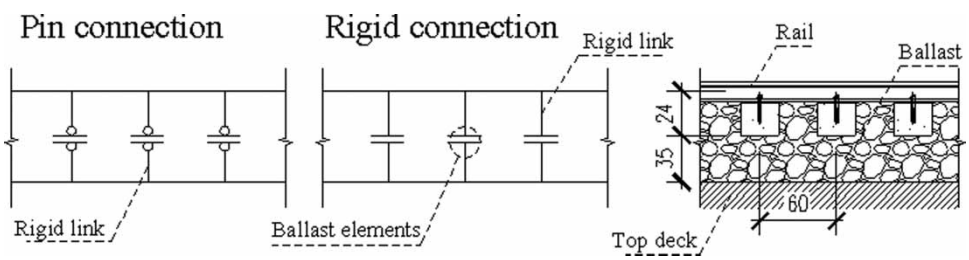

Fig. 4 FE schematization of deck–rail connection

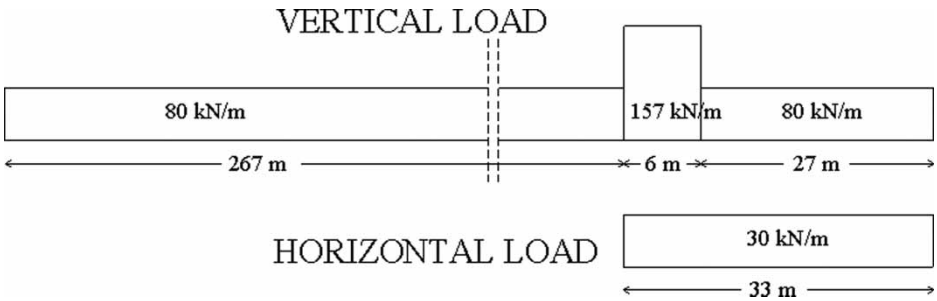

Fig. 5 The LM71 (UIC71) loading scheme

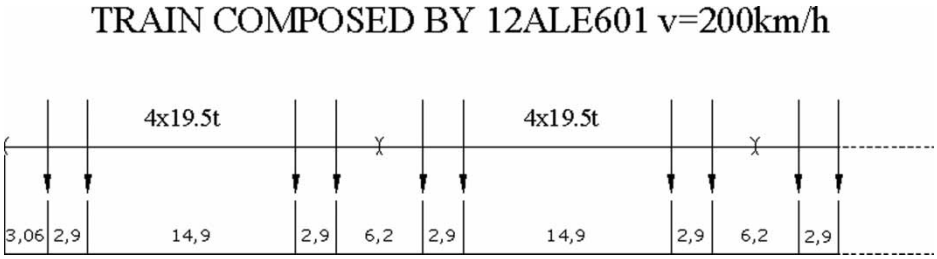

Fig. 6 The ALE601 train used for the resonance analysis

times the rail–pin distance. Assuming the rotation to take place mostly at the sleeper–ballast interface, the eccentricity of the axial load carried by the rails is around 20–25 cm. Consequently, if the deck rail connection of the FE model has a longitudinal spacing (d) larger then that of the sleepers (around 0.6 m), it is necessary to scale (increase) the rail bending stiffness (inertia). The rail equivalent inertia (I_{eq}) to be used in the model is found imposing the rotational flexibility of the rail element between adjacent ballast elements at a distance d to be equal to the rotational flexibility of the rail between two adjacent sleepers

$$I_{eq} = I_{rail} \times \left(\frac{d}{0.6}\right)^2 \tag{6}$$

6.3 The applied loadings

The analysis has been carried out by initially applying a regular increase in temperature to the deck of $\Delta T = 15\,^{\circ}\mathrm{C}$ and subsequently allowing the train (*LM71*) to run over the whole track length. Although with a single-track alignment, the model can still take two distinct trains running in opposite directions as generally required by the Italian Norm; again, for the sake of simplicity, a single accelerating train has been applied (Fig. 5). The 300 m long train, starts at abscissa $x = 0$ and terminates when the trailing cars are out of the model that means the total running length is 534.5 m. For the resonance analyses, the first of the five different trains specified by the Italian Norm has been used. This is made of 12 ALE601 cars running at up to 200 km/h with an interval of 10 km/h (Fig. 6).

7 THE RAIL–STRUCTURE INTERACTION

The most intuitive effect of rail–structure interaction is the horizontal force applied to the fixed support. With changing deck temperature, the rail pushes against the fixed support (Fig. 7). For a 34 m span, as the one under consideration, the force tends to an asymptote, which is attained when the ballast yields along the whole deck length. For this case, the ballast yield force over bridge has been assumed equal to that over soil at 12.5 kN/m (the same simplification is used in the blind tests required for validation by the Italian Railway agency) thus giving an asymptotic force of $F = 12.5 \times 34 = 425$ kN.

Figures 8 and 9 show the distribution of force and displacement, respectively, along the rail for a 15 °C temperature change. The maximum compression is

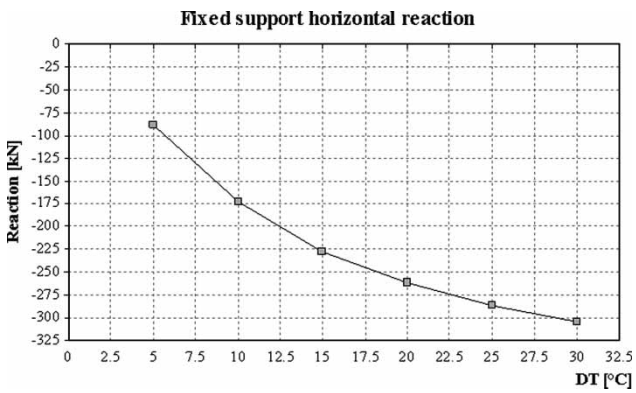

Fig. 7 Fixed support horizontal reaction

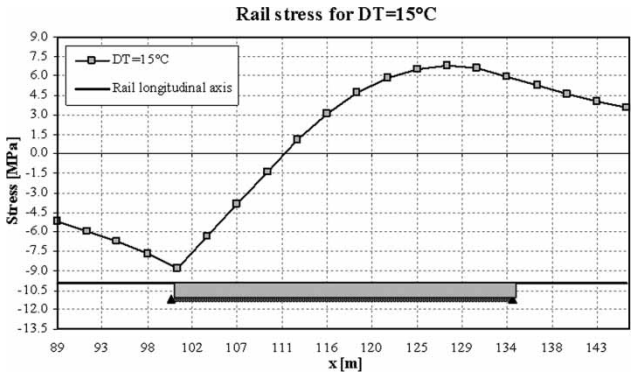

Fig. 8 Rail temperature stress

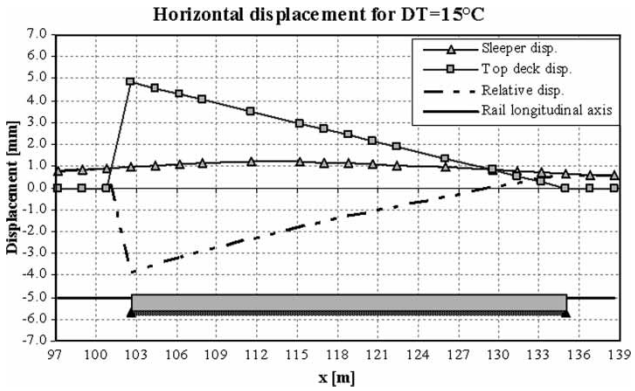

Fig. 9 Horizontal rail displacement due to temperature

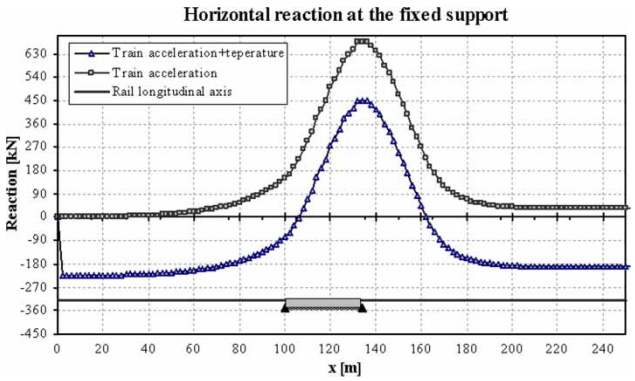

Fig. 10 Horizontal reaction time history

found at the sliding support (deck expansion joint) with $\sigma_c = -8.8$ MPa, and maximum tensile stress few metres ahead of the fixed support (on the deck) with $\sigma_t = 6.8$ MPa.

The time histories (THs) of the fixed support horizontal reaction due to the combined effect of temperature–train acceleration and train alone, are plotted in Fig. 10 as a function of the abscissa (x) to the front of the train. The maximum reaction takes place just before the train start to leave the deck at abscissa 134 m.

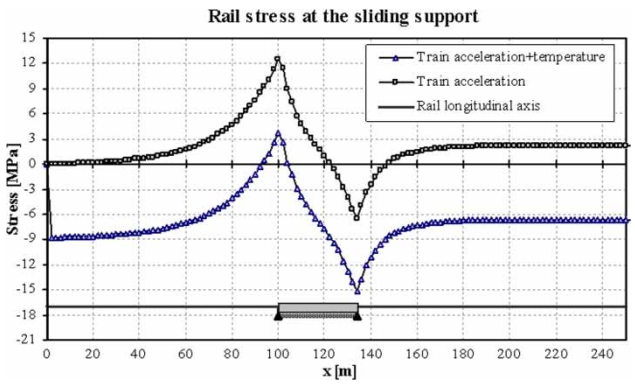

Fig. 11 Rail stress time history at the sliding support

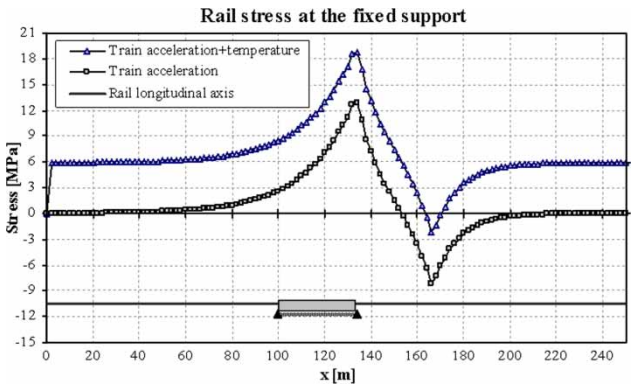

Fig. 12 Rail stress time history at fixed support

The TH of the rail stress above the sliding support is plotted in Fig. 11. The accelerating train pulls the rail until it reach the deck when it start to push it, adding this effect to the temperature, until the maximum value of $\sigma_c = -15.2$ MPa is found with the train when it leaves the deck (abscissa $x = 134$ m). The corresponding stress TH over the fixed support is plotted in Fig. 12.

The THs of the rail horizontal displacement to the ground at the sliding support ($x = 100$ m) are plotted in Fig. 13. The figure shows the rail displaced backwards by both temperature and the approach of the accelerating cars up to a maximum of 2.6 mm.

It is interesting to note that the rail remain displaced even after the train has run over the deck because of the permanent deformation in the ballast. This residual displacement is the cause for the residual tension in the rail shown in Figs 11 and 12. Subsequent trains do not cause further rail (permanent) displacement since once the accelerating/breaking and temperature forces have been spread, thanks to ballast yielding, over the necessary length, unloading and reloading branches are liner elastic.

Finally the horizontal displacement profile of the rail and deck at the instant of maximum relative displacement ($x = 118$ m) due to train alone is plotted in

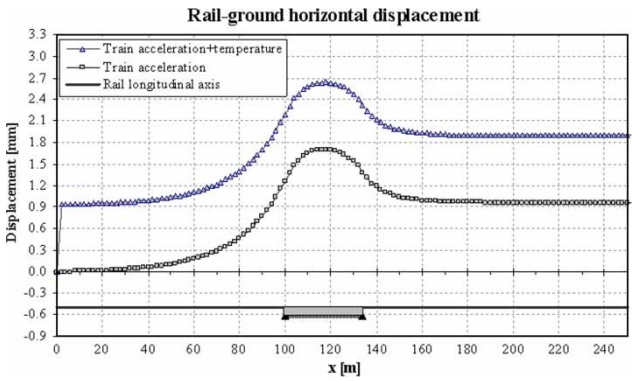

Fig. 13 Horizontal rail displacement time history

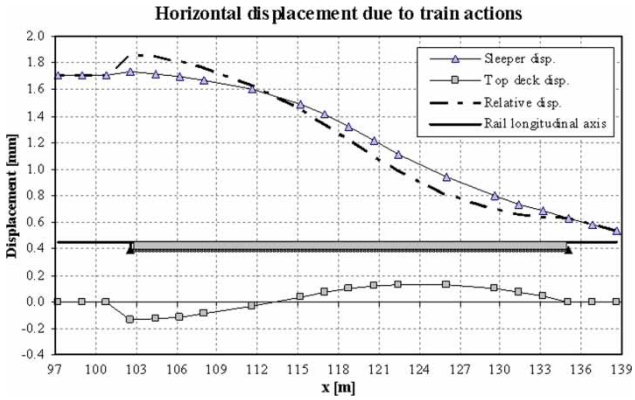

Fig. 14 Rail and deck horizontal displacements profile at maximum relative displacement

Fig. 14. The displacement of the deck is due to vertical bending and eccentricities of the supports, and to that of the rail is due to the accelerating force applied by the locomotive.

8 THE RESONANCE ANALYSIS

The same single box girder has been subjected to the ALE601 train running over it at an increasing speed up to 200 km/h. The real structure would effect couple bending and torsion because a single train would load it eccentrically. Since the first torsional frequency ($f_T = 9.86$ Hz) for the whole deck is more than 1.5 higher then the first bending one ($f_V = 4.61$ Hz), Italian Norm allows the use of a plane (two-dimensional) model ignoring the torsional effects. For each sampled speed, the dynamic amplification factor is plotted (Fig. 15) as the ratio of the maximum dynamic deflection over the static one. Three curves are plotted, the response of the structure with and without tracks, and the response of the structure without tracks but with a simplified input where the closely spaced (coupled) axels (2.9 m apart) have been merged into one.

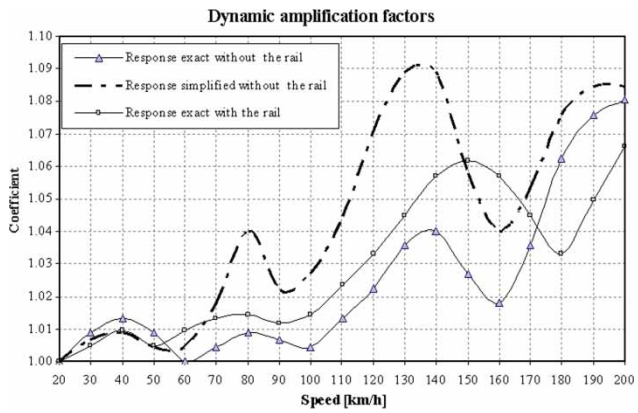

Fig. 15 Dynamic amplification factors

The figure shows the amplification factor for the girder under consideration to be relatively small. This is due to the weight of the structure (7500 kN for half deck) and to the very disperse frequency content of the train itself with single axel spacing varying from 2.9 to 14.9 m, and groups of closely spaced axels recurring every 9.1–26.9 m. As a matter of fact, by merging the adjacent axels, a significant increase in the amplification factor is observed (Fig. 15). When track is taken into account, the bridge frequencies increase and the (amplification factor) response curve is shifted towards higher speed/excitation frequencies.

Again, the results found for this specific and very simple bridge model are not applicable to other situations, although, the single span response may be representative of the bridge resonant behaviour while it is never so for the track–structure bridge response. It certainly is so for simply supported multiple spans as in this case, most frequent in Italy, each span behaves independently while for continuous girders, each span does influence the adjacent ones and therefore the complete bridge need to be modelled.

9 THE SEISMIC RESPONSE WITH AND WITHOUT CWR

Given the rail axial stiffness and the hysteretic behaviour of the ballast, a significant reduction of the bridge response under seismic input is expected when CWR is considered. Obviously, some bridge configurations under severe seismic input may cause the rail to buckle and therefore a strong reduction in the dissipating capacity of the ballast is expected. This aspect is addressed in a separate research by the authors [**12**], whereby using a large displacement analysis, it is demonstrated that buckling will only occur for very strong earthquake or very flexible structures.

In this work, an EC8 compatible, medium intensity accelerogram has been generated with a peak ground

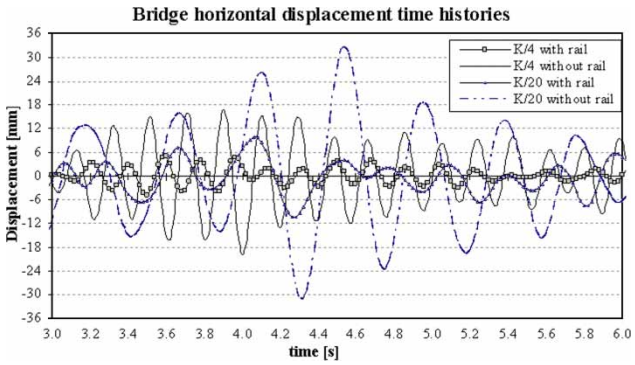

Fig. 16 Bridge horizontal displacement time histories

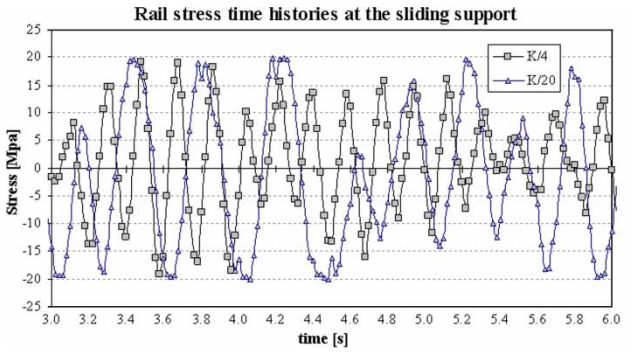

Fig. 17 Rail stress time histories at the sliding support

acceleration of 0.25 g. The structure with and without track has been subjected to this ground motion applied in the longitudinal direction (parallel to the track axis). In order to amplify the bridge response, the stiffness of the fixed support has been reduced by a factor of 4 and 20 with respect to the previous tests thus obtaining a stiffness corresponding roughly to 10 m high piers.

The long welded rail reduces the response (displacement of the fixed support) by 60 and 73 per cent, respectively (Fig. 16). These results are obtained for a maximum force in the rail, which is well below the buckling critical value as shown in Fig. 17. Maximum forces are also comparable for the to stiffness configurations since a complete yielding of the ballast over the deck is attained in both cases.

Finally, the hysteretic force–displacement response of a ballast element near the expansion joint (sliding support) is plotted (Fig. 18). The yielding force is equal to 7.5 kN, which is the maximum force transmissible by a single ballast element spaced at 0.6 m with a yield force of 12.5 kN/m ($F_y = 12.5 \times 0.6 = 7.5$ kN).

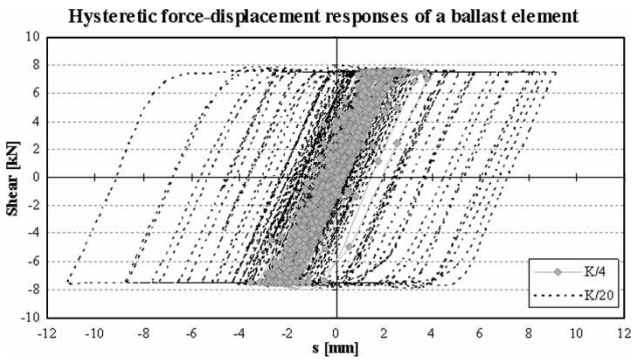

Fig. 18 Ballast force–displacement responses

10 CONCLUSION

Although the frictional behaviour of the ballast is quite simple and well understood, the interaction is less between the CWR and bridge girders when subjected to thermal and live loading. This interaction induces significant stresses in the rails but also modifies the response of railway bridges. Assessment of these phenomena can only be performed with non-linear FE analysis since there exists too many problem variables to be dealt with, making simplified approaches often unreliable. The FE model presented in this paper can simulate the principal mechanisms of track–structure interaction in the static and dynamic regime providing both an interesting insight to the response of railway bridges and a reliable estimate of the maximum stresses that can arise in the rail under different bridge configurations and external actions, including seismic input.

To this extent, the very simple case study presented cannot be extrapolated to other common situations, such as, for example, multiple spans, slender piers, uneven stiffness distribution among the different supports, and frictional or gap behaviour of the bearings and expansion joints. These situations arise when designing new structures as well as in the assessment of existing ones for rehabilitation and retrofitting purposes. They can be addressed only by using the intrinsic flexibility of the FE method once appropriate models have been understood, tested, and validated.

REFERENCES

1 **Istruzione, F. S.** Sovraccarichi per il calcolo dei ponti ferroviari. Istruzioni per la progettazione, l'esecuzione e il collaudo, 13 January, 1997, No. I/SC/PS-OM/2298.

2 **Conti, P. A.** La triade treno-binario-struttura. Problematiche considerazioni – sviluppi. Ingegneria Ferroviaria, CIFI, September 1992.

3 **Mondkar, D. P.** and **Powell, G. H.** Static and dynamic analysis of nonlinear structures. Report No. UCB/EERC-75/10, University of California, Berkeley, 1975.

4 **Petrangeli, M.** and **Ciampi, V.** Equilibrium based numerical solutions for the nonlinear beam problem. *Int. J. Numer. Methods Eng.*, 1996, **40**(3), 423–438.

5 **Petrangeli, M., Pinto, P. E.,** and **Ciampi, V.** A fibre element for cyclic bending and shear. Parts I and II. *ASCE, J. Eng. Mech.*, 1999, **125**(9), 994–1009.

6 **CEN EUROCODE 2.** Design of concrete structures. UNI-ENV-1992–1.

7 **CEN EUROCODE 8.** Design provisions for earthquake resistance of structures. UNI-ENV 1998-2: Bridges.

8 **BSSc.** NEHRP guidelines for the seismic rehabilitation of buildings. FEMA-273, Developed by ATC for FEMA, Washington, D.C., 1997.

9 **SEAOC.** *Vision 2000. Performance based seismic engineering of buildings*, Structural Engineers Association of California, Sacramento, 1995.

10 **Petrangeli, M., Andreocci, C., Magnorfi, F., Orlandini, M.,** and **Geremia, G.** Large concrete precast box girders along the new Italian high speed railway. In 7th International Conference on Short and Medium Span Bridges, IABSE, Montréal, 23–25 August, 2006, NC-016.

11 **Petrangeli, M., Andreocci, C., Leoncini, A., Orlandini, M.,** and **Geremia, G.** Il Bicassone Prefabbricato lungo la nuova linea Alta Capacita Torino-Milano. IIC Industria Italiana del Cemento, AITEC, January 2007, Vol. 827, pp. 64–77.

12 **Petrangeli, M., Tamagno, C.,** and **Tortolini, P.** L'interazione binario-struttura nella risposta sismica degli impalcati da ponte ferroviari in presenza di lunga rotaia saldata. Ingegneria Ferroviaria, CIFI, September 2007, pp. 857–874.

APPENDIX

Notation

d	longitudinal spacing
$\mathbf{D}$	compatibility matrix
f_{T}	torsional frequency
f_{V}	bending frequency
F_{min}	minimum friction force
F_{Y}	yield force
$\boldsymbol{F}^{\mathrm{e}}$	nodal forces
I_{eq}	equivalent inertia
K	tangent modulus
N	axial load
$\boldsymbol{U}^{\mathrm{e}}$	vector of nodal displacement
x	abscissa
Δ_{y}	yield displacement
ΔT	regular increase in temperature to the deck
ε^{e}	element generalized deformation
σ_{c}	compression stress
σ_{t}	tensile stress
Φ	friction coefficient